Increased efficiency in pn-junction PbS QD solar cells via NaHS treatment of the p-type layer

Speirs, Mark J.; Balazs, Daniel M.; Dirin, Dmitry N.; Kovalenko, Maksym V.; Loi, Maria Antonietta

Published in:
Applied Physics Letters

DOI:
10.1063/1.4978444

Increased efficiency in pn-junction PbS QD solar cells via NaHS treatment of the p-type layer

Mark J. Speirs, Daniel M. Balazs, Dmitry N. Dirin, Maksym V. Kovalenko, and Maria Antonietta Loi

Citation: Appl. Phys. Lett. **110**, 103904 (2017); doi: 10.1063/1.4978444
View online: http://dx.doi.org/10.1063/1.4978444
View Table of Contents: http://aip.scitation.org/toc/apl/110/10
Published by the American Institute of Physics

Increased efficiency in pn-junction PbS QD solar cells via NaHS treatment of the p-type layer

Mark J. Speirs,[1] Daniel M. Balazs,[1] Dmitry N. Dirin,[2,3] Maksym V. Kovalenko,[2,3] and Maria Antonietta Loi[1,a)]

[1]*Photophysics and OptoElectronics, Zernike Institute for Advanced Materials, University of Groningen, Nijenborgh 4, Groningen 9747 AG, The Netherlands*

[2]*Department of Chemistry and Applied Biosciences, ETH Zürich, Wolfgang-Pauli-Str. 10, Zürich 8093, Switzerland*

[3]*EMPA-Swiss Federal Laboratories for Materials Science and Technology, Überlandstr. 129, Dübendorf 8600, Switzerland*

(Received 10 January 2017; accepted 28 February 2017; published online 9 March 2017)

Lead sulfide quantum dot (PbS QD) solar cell efficiencies have improved rapidly over the past years due in large part to intelligent band alignment considerations. A pn-junction can be formed by connecting PbS layers with contrasting ligands. However, the resulting doping concentrations are typically low and cannot be effectively controlled. Here, we present a method of chemically p-doping films of thiol capped PbS QDs. P-n junction solar cells with increased doping in the p-type layer show improved short circuit current and fill factor, leading to an improvement in the power conversion efficiency from 7.1% to 7.6%. By examining Schottky diodes, field effect transistors, and the absorption spectra of treated and untreated PbS QDs, we show that the improved efficiency is due to the increased doping concentration in the thiol capped QD layer and to denser packing of the PbS QD film. *Published by AIP Publishing.* [http://dx.doi.org/10.1063/1.4978444]

Over the last decade, lead sulfide quantum dots (PbS QDs) have been a topic of great interest in the field of solution processable photovoltaics.[1] Their success stems in part from the large (18 nm) Bohr radius of PbS,[2] which leads to a broadly tunable bandgap for QDs in the size range 3–5 nm, and in part from the electronic adaptability offered by the large library of ligands that are able to modify the QD surface. This not only allows control over charge carrier mobility but also allows control of the conduction and valence levels with respect to the vacuum level, as well as the position of the Fermi energy level within the bandgap.[3] Clever implementation of these versatile characteristics has driven the steady increase in power conversion efficiency (PCE) to more than 10% to date.[4] The most efficient device structures currently feature a junction between an n-type layer of PbS, treated with tetrabutylammonium iodide (TBAI), and a layer of ethanedithiol (EDT) capped PbS.[4–6] The alignment of the Fermi levels across the junction gives rise to a built in electric field, which induces a beneficial band-bending and facilitates drift driven charge extraction.[6]

Nevertheless, PbS QD solar cells still fall well short of their potential, in particular, due to a low fill factor (FF) and an open circuit voltage (V_{OC}) that falls well below the theoretical limit.[7,8] In our previous work, we demonstrated that these solar cells can benefit from an increased doping concentration in the EDT layer.[6] Due to charge conservation across the pn-junction, the distribution of the depletion region across the junction is governed by

$$N_D w_D = N_A w_A, \tag{1}$$

with $N_{D(A)}$ the doping concentration of the n(p)-type layer and $w_{D(A)}$ the fraction of the depletion region located on the n(p)-type side. Thus, the increased doping in the EDT layer would shift the distribution of the depletion region towards the TBAI layer, which has higher charge carrier mobility,[6] and would thus facilitate more efficient charge extraction.

Many doping strategies have been demonstrated for lead chalcogenide QDs.[9] These include doping via oxidation,[10–15] ligand control,[3,12,16,17] stoichiometry and defects,[18–20] and heterovalent impurities.[21–23] While n-type films have been fabricated through ligands such as hydrazine and halide salts,[17,24] p-type doping of thiol capped films has so far mostly been achieved via oxidation in ambient conditions. That doping strategy has been used explicitly by Choi *et al.*[14] in Schottky solar cells, and implicitly in pn-junction devices which have been exposed to air during or after the deposition of the thiol capped layer.[5,25] Bawendi *et al.* reported that pn-junction devices stored in air can display an initial increase in the efficiency, which can be attributed to the increased doping of the EDT capped layer.[5] Nevertheless, oxidative doping is not well controlled, and while oxygen is effective in shifting the Fermi level, the unavoidable adsorption of other atmospheric contaminants, in particular, water, to the PbS surface is likely to have a detrimental effect on trap densities and charge carrier mobilities. Therefore, a more controlled and systematic method of p-doping is desirable. On the contrary, tuning of the stoichiometry of lead chalcogenide QDs has been demonstrated to be a controllable method of tuning the Fermi level in lead chalcogenide QDs. Kagan *et al.* showed that thermally evaporating excess Pb on to PbSe QD films enhances the n-type behaviour and, similarly, more p-type behaviour was achieved by evaporating excess Se.18 However, it is desirable to achieve the same effect via solution processable techniques, compatible with cheap and large scale production methods. Kagan *et al.*

a)Author to whom correspondence should be addressed. Electronic mail: m.a.loi@rug.nl

also reported an increase in the solar cell efficiency using a combination of thiocyanate (SCN) and 1,4-benzenedithiol (BDT) ligands.[26] In that work, the solar cells treated with both BDT and SCN exhibited a modest efficiency of 3.5%, compared to 2.1% for solar cells treated with only BDT. It was also noted that this method was limited to active layers less than 150 nm thick, as the poor resulting mobility hinders charge extraction in thicker films. Chalcogenide salts such as Na_2S, Na_2Se, and K_2S are soluble in polar solvent and have been demonstrated to effectively alter the PbS, PbSe, or CdSe stoichiometry and increased p-type doping in transistors, leading to higher p-type currents and charge carrier mobilities in field effect transistors.[26–30] However, the success of these salts in solar cell structures has been limited, likely due to the extremely high reactivity of these salts, which can introduce trap states into the film and cause a pronounced fusion of the QDs, leading to a lower V_{OC}.

In this work, we fabricate efficient pn-junction solar cells using TBAI treated PbS as n-type layer and EDT capped PbS as p-type layer. We report a simple and reproducible method of p-doping thiol capped PbS films by post deposition treatment with a solution of sodium hydrosulfide (NaHS). NaHS is chosen because the HS^- anion is expected to produce a milder reaction compared to chalcogenic salts such as Na_2S. In addition, NaHS is more soluble than the chalcogenic alternatives, which facilitates the fabrication process. We show an increase in the short circuit current (J_{SC}) and FF for pn-junction QD solar cells without detriment to the V_{OC}, leading to an improvement in the PCE from 7.1% to 7.6%. We then fabricate Schottky diodes with various concentrations of doping. The doping concentration is measured via Mott-Schottky analysis and found to increase by more than a factor of 3. Under illumination, decreasing J_{SC} of the Schottky devices is observed with increasing doping concentration, which can be explained by a narrowing of the depletion region near the Schottky junction due to increased doping. We see no change in the V_{OC} or FF, indicating that the doping procedure has little effect on charge transport properties or recombination rates. Finally, the absorption spectra reveal only a very small loss in quantum confinement upon NaHS treatment.

PbS QDs capped with oleic acid are synthesized using a previously reported method.[31] The QDs exhibit a first excitonic peak at 860 nm, corresponding to a bandgap of 1.44 eV (Figure S1 of the supplementary material). A compact film of anatase TiO_2 is prepared by spincasting a 20:2:1 solution of ethanol:titanium(IV) butoxide:HCl onto pre-patterned fluorine doped tin-oxide substrates (13 Ω/sq) and annealed at 450 °C for 30 min. The n-type PbS film is deposited by spincoating a 10 mg/ml solution of PbS layer-by-layer in hexane, by exposure of the film to 15 mg/ml TBAI in methanol followed by spindrying and two washing steps with pure methanol to remove the tetrabutylammonium cation. The p-type layer is formed by spincoating, followed by the exposure of a 0.01% $\frac{v}{v}$ EDT in acetonitrile and one washing step with acetonitrile. For the doped samples, each layer was exposed to a 0.1 mM solution of NaHS in MeOH for 15 s after the EDT treatment and prior to the washing step. The high reactivity of NaHS and the low concentration used here together prevent the penetration of NaHS into the TBAI capped film, where the p-doping effect would have a detrimental effect. The higher concentrations of NaHS also often led to the delamination of the active layer. The active layer comprises 12 layers (~200 nm) of TBAI and 4 layers (~60 nm) of EDT capped PbS. Since some degree of oxidative doping is unavoidable, we choose to expose all the devices to air prior to the deposition of the electrodes to ensure that any effect we see is in addition to the oxidative doping.

The devices are finished by thermal evaporation of 5 nm MoO_3 and 80 nm of Au. Here, we would like to comment on the use of MoO_3 as a hole extracting layer, since there are conflicting reports concerning the use of MoO_3 in the literature. Some authors have reported high efficiencies using only Au as a top electrode,[4,5] and reported a decreased stability when MoO_3 is used.[5] Other studies have chosen to include MoO_3 as part of the anode,[32–34] and Sargent *et al.* have reported that a detrimental Schottky barrier is formed at the PbS/Au interface,[35] which can be removed by using MoO_3 as an interlayer.[36] In our case, devices without MoO_3 have an impractically low yield of non-shorted devices, possibly due to the penetration of Au clusters into the active layer during thermal deposition, which the MoO_3 is able to prevent. Therefore, we have chosen to include MoO_3 both as a hole transporting layer and as protection for the active layer from the electrode deposition.

The current-voltage ($J - V$) curves of representative doped and undoped device are shown in Figure 1, and the main parameters are shown in Table I. In total, 13 devices on 4 independent substrates were made for the undoped case and 11 devices over 4 substrates for the doped case. To avoid the inclusion of shorted or almost shorted devices, only solar cells with a high rectification ratio in the dark $\left(\frac{J_{|V=1}}{J_{|V=-1}} > 100\right)$ were included in the dataset. The doped solar cells show small but consistent increases in J_{SC}, from 26.0 to 27.0 mA/cm^2, and FF, from 0.49 to 0.51, with a practically unchanged V_{OC}, leading to an average increase in PCE from 7.1% to 7.6%. The external quantum efficiency (EQE) spectra are shown in Figure S2 (supplementary material); the current calculated by integrating the product of the EQE spectrum with the AM1.5G solar spectrum corresponds well to the current obtained in the $J - V$ curves.

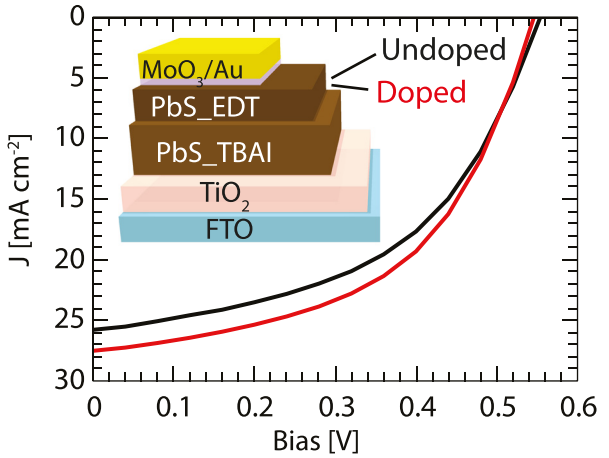

FIG. 1. Representative JV curves of pn-junction solar cell with doped (red) and undoped (black) PbS_EDT layers. The device structure is shown in the inset.

TABLE I. $J-V$ parameters with doped and undoped PbS_EDT layers. The values in brackets give the standard deviation over the dataset.

Device	J_{SC} [mA/cm^2]	V_{OC} [V]	FF	PCE [%]
Best undoped device	26.4	0.56	0.53	8.1
Best doped device	27.4	0.55	0.56	8.6
Undoped average	26.0(±0.8)	0.56(±0.01)	0.49(± 0.02)	7.1(±0.6)
Doped average	27.0(±0.4)	0.55(±0.01)	0.51(±0.03)	7.6(±0.6)

To determine the reason for this improvement, the PbS_EDT layer is examined independently. To this end, Schottky diodes are fabricated by depositing 150–180 nm PbS_EDT on pre-patterned indium tin oxide (ITO) and finished with 1 nm of LiF and 100 nm aluminium. The parallel plate capacitance C is measured as a function of bias in the dark; a 25 mV ac signal with a frequency of 250 Hz was superimposed on a forward bias ranging from −0.5 V to 0.5 V. The resulting $C-V$ plots are shown in Figure 2. The doping concentration N can be obtained using the Mott-Schottky equation,

$$\frac{A^2}{C^2} = \frac{2}{q\epsilon_r\epsilon_0 N}\left(V - V_{bi} - \frac{kT}{q}\right), \tag{2}$$

where A is the device area, ϵ_r and ϵ_0 are the relative and vacuum permittivities, respectively, V_{bi} is the built in voltage, k is Boltzmann's constant, T is the temperature, and e is the elementary charge. In the voltage range where the depletion region depends on the applied bias, the Mott-Schottky curve is linear, and a doping concentration of 1.9×10^{16} cm^{-3} is found for the undoped film while the film doped with NaHS shows a more than threefold higher doping concentration of 6.5×10^{16} cm^{-3}. In light of this, the V_{OC} of these solar cells is expected to increase by approximately 28 mV due to the increased built in bias over the pn-junction according to

$$V_{bi} = \frac{kT}{q}\ln\left(\frac{N_A N_D}{n_i^2}\right). \tag{3}$$

Since this increase is not observed, it must be negated by either increased charge carrier recombination or a lower bandgap.

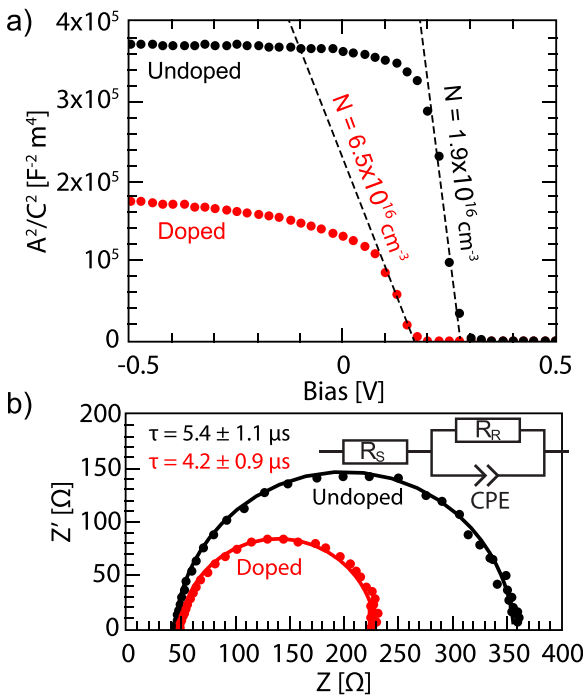

FIG. 2. Voltage dependent capacitance extracted from impedance spectra in the dark for doped (red) and undoped (black) PBS_EDT. (b) Nyquist impedance spectra of doped and undoped films under 1 Sun illumination, held at open circuit voltage.

The charge carrier lifetime plays a crucial role in the device performance. Increasing the density of states within the bandgap can potentially assist the detrimental recombination processes leading to a reduced charge carrier lifetime. To illucidate the role this doping method has on the recombination rates of minority charge carriers, in this case electrons, impedance spectra were obtained while holding the diodes at open circuit bias under 1 Sun illumination. Because no current flows through the device at open circuit bias, all photogenerated charge carriers must necessarily recombine. The typical rate at which the recombination takes place can be found from $\tau = R_r C_r$,[31] where R_r is the recombination resistance and C_r is the capacitance found by fitting the Nyquist plots with the equivalent circuit consisting of a constant phase element (Q) in parallel with the recombination resistance and a series resistance, see the inset in Figure 2(b). The constant phase element takes into account the slightly depressed impedance spectra, which can be explained by small inhomogeneities such as roughness or pinholes at the electrode interface.[37] The fitting parameter a indicating the deviation from an ideal capacitor is 0.96 for these devices, indicating almost ideal capacitance behaviour. The capacitance is calculated from the constant phase element using the relationship $C_{eq} = Q(2\pi f_{peak})^{a-1}$,[38] where f_{peak} is the frequency at the peak maximum imaginary component of the Nyquist spectrum. With this method, carrier lifetimes of 5.4 ± 1.1 μs for the undoped film are almost equal to the value of 4.2 ± 0.9 μs found for the film doped with NaHS. These values are comparable to the values obtained by the alternative method $\tau = 1/(2\pi f_{peak})$,[31] which gives values of 5.0 ± 0.6 μs for the undoped film and 4.4 ± 0.5 μs for the undoped film. The close similarity in lifetimes indicates that the doping process does not affect the recombination rates under normal operating conditions.

$J-V$ curves of three Schottky diodes fabricated with NaHS concentrations of 0, 0.02, and 0.1 mM were measured under 1 Sun illumination to further investigate the effect of NaHS doping on the properties of PbS_EDT films. The curves are shown in Figure 3, and the solar cell parameters are shown in Table II. The J_{SC} decreases with increasing doping, while the V_{OC} and FF are both unchanged. Charge extraction in Schottky solar cells is limited by diffusion of the charge carriers towards the Schottky barrier,[39] in this case the aluminium contact, where energy level bending drives the separation of electrons and holes to their respective electrodes. For a Schottky junction, the width of the region in which band bending exists is given by[40]

$$w = \left[\frac{2\varepsilon_0\varepsilon_r}{qN}\left(V_{bi} - V - \frac{kT}{q}\right)\right]^{1/2}, \tag{4}$$

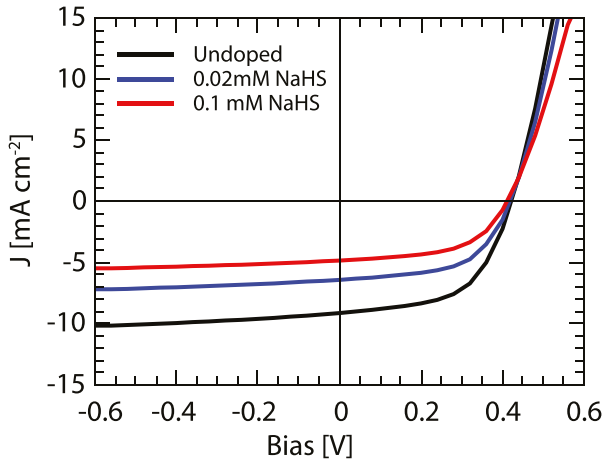

FIG. 3. $J - V$ curves for Schottky solar cells exposed to 0.1 mM NaHs (blue), 0.02 mM NaHS (red), and without additional doping (black).

thus the decreasing J_{SC} can be attributed to the narrowing of the depletion region, caused by the increased doping concentration. The constant V_{OC} is another indication that the doping mechanism does not significantly alter the trap density or charge carrier lifetimes, while the unchanged FF indicates that the doping mechanism does not significantly improve or impair charge extraction. The ideality factor n was then calculated from the dependence of the V_{OC} on the light intensity I (Figure S3 of the supplementary material)

$$V_{OC} = \frac{nkT}{q} \ln\left(\frac{J_{PH}}{J_0}\right), \tag{5a}$$

$$= \frac{nkT\alpha}{q} \ln(I) + c, \tag{5b}$$

where k is Boltzmann's constant, T is the temperature, q is the elementary charge, α is an empirical parameter indicating the linearity of the photocurrent with intensity ($J_{PH} \propto I^{\alpha}$), and c is a fitting parameter collecting all the terms independent of light intensity. For the undoped films, an ideality factor of 1.50 is found, while for the doped film a similar value of 1.57 is found. An ideality factor of 1 corresponds to fully bimolecular recombination, while an ideality factor of 2 means that the trap assisted recombination is the dominating mechanism. The similar values of n confirm that NaHS does not introduce a significant amount of traps or alter the main recombination processes.

To investigate the effect of NaHS treatment on the charge transport properties, SiO_2-gated field effect transistors (FETs) were fabricated with films prepared in the same manner as the solar cells. For NaHS treated films, a significantly higher current is observed in both the output and transfer curves in the p-channel (Figure S4 of the supplementary material), leading to a slightly increased hole mobility of 1.3×10^{-5} cm^2/Vs for the treated device, compared to 5.0×10^{-6} cm^2/Vs for the control device. This is either due to the higher charge carrier concentration as a result of the increased doping or due to the denser packing of the NaHS treated film (see below).

TABLE II. $J - V$ parameters with doped and undoped PbS_EDT layers.

Device	J_{SC} [mA/cm^2]	V_{OC} [V]	FF	PCE [%]
Undoped	9.1	0.42	0.56	2.3
0.02 mM NaHS	6.4	0.41	0.54	1.4
0.1 mM NaHS	4.8	0.41	0.54	1.1

Finally, from the absorption spectrum in Figure 4, we see a small redshift of the treated QDs from 915 nm to 940 nm, corresponding to a difference in the bandgap of 36 meV, which could indicate slightly denser packing, leading to a partial loss of quantum confinement coupled with higher film conductivity, in agreement with the FET measurements. The decrease in the bandgap is close to the 28 meV increase in V_{OC} expected from a threefold increase in the p-type doping concentration. The two effects likely cancel out, resulting in a significant effect only for the J_{SC} and FF. The effect of the increased doping concentration, improved conductivity, and lower bandgap can contribute to the observed increases in J_{SC} and FF. However, the effect of the improved hole mobility and bandgap are likely small since both these effects should lead to increased J_{SC} in the Schottky devices as well as the pn-junction solar cells. Instead, the J_{SC} of the Schottky devices decreases with more NaHS treatment, indicating that they are dominated by the decreased depletion width caused by higher doping.

In conclusion, we have shown an average performance improvement of 0.5 percentage points in efficient pn-junction QD solar cells using a facile treatment of the p-type layer with NaHS. The improvement is due to small increases in both J_{SC} and FF, without the degradation of the V_{OC}. The treated films exhibit a threefold increase in the doping concentration, without the loss of charge carrier lifetime. The expected increase of 28 meV in the V_{OC} from the increased doping is compensated by the slight loss of quantum confinement after NaHS treatment leading to a 36 meV lower bandgap. We have shown that the change in J_{SC} and FF is due to both the increased doping concentration, which shifts the depletion region towards the TBAI capped PbS layer, and due to the lower bandgap and higher film conductivity. We would like to note that an even higher doping concentration would be desirable to further decrease the necessary thickness of the p-type layer, similar to the strategy used in many silicon solar cells, where a thick low doping

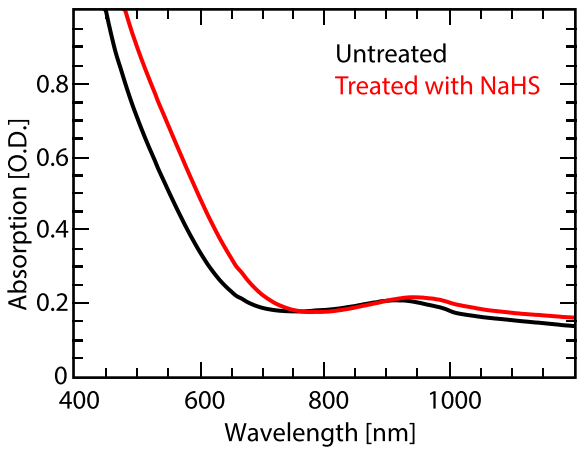

FIG. 4. Absorption spectrum of untreated (black) and NaHS treated (red) PbS QD films.

concentration (usually p-type) layer is used in combination with a thin highly doped (n-type) layer. In this case, we were limited by the mechanical stability of our active layer, which exhibited frequent delamination when exposed to higher concentrations of NaHS in methanol. Further increasing the doping concentration of the p-type layer is expected to yield even better results.

See supplementary material for detailed fabrication methods, the absorption, and PL spectra of the QDs, EQE spectrum, ideality factor data, and FET measurements.

M. J. Speirs and M. A. Loi acknowledge the financial support of the Alumnikring Den Haag/Rotterdam through the Ubbo Emmius Fund of the University of Groningen. We thank Lu Han for the help with the transistor measurements. M.A.L. acknowledges also the support of the ERC Starting Grant "Hybrids Solution Processable Optoelectronic Devices" (Hy-SPOD) (ERC-306983); M. V. Kovalenko acknowledges the partial financial support from ERC Starting Grant NANOSOLID (GA No.306733).

[1]M. V. Kovalenko, Nat. Nanotechnol. **10**, 994 (2015).
[2]F. Wise, Acc. Chem. Res. **33**, 773 (2000).
[3]P. R. Brown, D. Kim, R. R. Lunt, N. Zhao, M. G. Bawendi, J. C. Grossman, and V. Bulović, ACS Nano **8**, 5863 (2014).
[4]X. Lan, O. Voznyy, F. P. Garcia de Arquer, M. Liu, J. Xu, A. H. Proppe, G. Walters, F. Fan, H. Tan, M. Liu, Z. Yang, S. Hoogland, and E. H. Sargent, Nano Lett. **16**(7), 4630–4634 (2016).
[5]C.-H. M. Chuang, P. R. Brown, V. Bulović, and M. G. Bawendi, Nat. Mater. **13**, 796 (2014).
[6]M. J. Speirs, D. N. Dirin, M. Abdu-Aguye, D. M. Balazs, M. V. Kovalenko, and M. A. Loi, Energy Environ. Sci. **9**, 2916 (2016).
[7]C.-H. M. Chuang, A. Maurano, R. E. Brandt, G. W. Hwang, J. Jean, T. Buonassisi, V. Bulović, and M. G. Bawendi, Nano Lett. **15**, 3286 (2015).
[8]A. Polman, M. Knight, E. C. Garnett, B. Ehrler, and W. C. Sinke, Science **352**(6283) (2016).
[9]A. Stavrinadis and G. Konstantatos, ChemPhysChem **17**, 632 (2016).
[10]E. J. Klem, H. Shukla, S. Hinds, D. D. MacNeil, L. Levina, and E. H. Sargent, Appl. Phys. Lett. **92**, 212105 (2008).
[11]D. M. Balazs, M. I. Nugraha, S. Z. Bisri, M. Sytnyk, W. Heiss, and M. A. Loi, Appl. Phys. Lett. **104**, 112104 (2014).
[12]O. Voznyy, D. Zhitomirsky, P. Stadler, Z. Ning, S. Hoogland, and E. H. Sargent, ACS Nano **6**, 8448 (2012).
[13]G. Konstantatos, L. Levina, A. Fischer, and E. H. Sargent, Nano Lett. **8**, 1446 (2008).
[14]M.-J. Choi, J. Oh, J.-K. Yoo, J. Choi, D. Sim, and Y. S. Jung, Energy Environ. Sci. **7**, 3052 (2014).
[15]S. J. Oh, C. Uswachoke, T. Zhao, J.-H. Choi, B. T. Diroll, C. B. Murray, and C. R. Kagan, ACS Nano **9**, 7536 (2015).
[16]A. H. Ip, S. M. Thon, S. Hoogland, O. Voznyy, D. Zhitomirsky, R. Debnath, L. Levina, L. R. Rollny, G. H. Carey, A. Fischer, K. W. Kemp, I. J. Kramer, Z. Ning, A. J. Labelle, K. W. Chou, A. Amassian, and E. H. Sargent, Nat. Nano. **7**, 577 (2012).
[17]D. Zhitomirsky, M. Furukawa, J. Tang, P. Stadler, S. Hoogland, O. Voznyy, H. Liu, and E. H. Sargent, Adv. Mater. **24**, 6181 (2012).
[18]S. J. Oh, N. E. Berry, J.-H. Choi, E. A. Gaulding, T. Paik, S.-H. Hong, C. B. Murray, and C. R. Kagan, ACS Nano **7**, 2413 (2013).
[19]J. M. Luther and J. M. Pietryga, ACS Nano **7**, 1845 (2013).
[20]D. Kim, D.-H. Kim, J.-H. Lee, and J. C. Grossman, Phys. Rev. Lett. **110**, 196802 (2013).
[21]J. Liu, Q. Zhao, J.-L. Liu, Y.-S. Wu, Y. Cheng, M.-W. Ji, H.-M. Qian, W.-C. Hao, L.-J. Zhang, X.-J. Wei, S.-G. Wang, J.-T. Zhang, Y. Du, S. X. Dou, and H.-S. Zhu, Adv. Mater. **27**, 2753 (2015).
[22]H. Liu, D. Zhitomirsky, S. Hoogland, J. Tang, I. J. Kramer, Z. Ning, and E. H. Sargent, Appl. Phys. Lett. **101**, 151112 (2012).
[23]A. Stavrinadis, A. K. Rath, F. P. G. de Arquer, S. L. Diedenhofen, C. Magén, L. Martinez, D. So, and G. Konstantatos, Nat. Commun. **4**, 2981 (2013).
[24]D. V. Talapin and C. B. Murray, Science **310**, 86 (2005).
[25]M. Yuan, O. Voznyy, D. Zhitomirsky, P. Kanjanaboos, and E. H. Sargent, Adv. Mater. **27**, 917 (2015).
[26]S. Oh, D. Straus, T. Zhao, J.-H. Choi, S.-W. Lee, E. Gaulding, C. Murray, and C. Kagan, Chem. Commun. **53**, 728 (2017).
[27]E. Goodwin, D. B. Straus, E. A. Gaulding, C. B. Murray, and C. R. Kagan, Chem. Phys. **471**, 81 (2016).
[28]Y. Liu, J. Tolentino, M. Gibbs, R. Ihly, C. L. Perkins, Y. Liu, N. Crawford, J. C. Hemminger, and M. Law, Nano Lett. **13**, 1578 (2013).
[29]D. K. Kim, A. T. Fafarman, B. T. Diroll, S. H. Chan, T. R. Gordon, C. B. Murray, and C. R. Kagan, ACS Nano **7**, 8760 (2013).
[30]A. Nag, M. V. Kovalenko, J.-S. Lee, W. Liu, B. Spokoyny, and D. V. Talapin, J. Am. Chem. Soc. **133**, 10612 (2011).
[31]L.-H. Lai, L. Protesescu, M. V. Kovalenko, and M. A. Loi, Phys. Chem. Chem. Phys. **16**, 736 (2014).
[32]T. Zhao, E. D. Goodwin, J. Guo, H. Wang, B. T. Diroll, C. B. Murray, and C. R. Kagan, ACS Nano **10**, 9267 (2016).
[33]A. Rath, F. P. García de Arquer, A. Stavrinadis, T. Lasanta, M. Bernechea, S. L. Diedenhofen, and G. Konstantatos, Adv. Mater. **26**, 4741 (2014).
[34]K. W. Kemp, A. J. Labelle, S. M. Thon, A. H. Ip, I. J. Kramer, S. Hoogland, and E. H. Sargent, Adv. Energy Mater. **3**, 917 (2013).
[35]L. Hu, A. Mandelis, X. Lan, A. Melnikov, S. Hoogland, and E. H. Sargent, Sol. Energy Mater. Sol. Cells **155**, 155 (2016).
[36]P. R. Brown, R. R. Lunt, N. Zhao, T. P. Osedach, D. D. Wanger, L.-Y. Chang, M. G. Bawendi, and V. Bulović, Nano Lett. **11**, 2955 (2011).
[37]B. Hirschorn, M. E. Orazem, B. Tribollet, V. Vivier, I. Frateur, and M. Musiani, Electrochim. Acta **55**, 6218 (2010).
[38]C. Hsu and F. Mansfeld, Corrosion **57**, 747 (2001).
[39]K. Szendrei, M. Speirs, W. Gomulya, D. Jarzab, M. Manca, O. V. Mikhnenko, M. Yarema, B. J. Kooi, W. Heiss, and M. A. Loi, Adv. Funct. Mater. **22**, 1598 (2012).
[40]S. M. Sze and K. K. Ng, *Physics of Semiconductor Devices* (Wiley, Hoboken, NJ, USA, 2007).